A CAMERA ORIENTATING DEVICE USING COMPLIANT MECHANISM FOR AUTONOMOUS MOBILE ROBOTS

Ngoc-Phuong Hoang[1], Quoc-Van Nguyen[2], Huy-Tuan Pham[1]*
[1]Ho Chi Minh City University of Technology and Education, Vietnam
[2]Cao Thang Technical College, Vietnam

Received 12/02/2019, Peer-reviewed 23/3/2019, Accepted for publication 02/4/2019

ABSTRACT

This paper presents the design of a compliant bio-inspired camera-positioning mechanism. The device combines human muscle actuation scheme and spherical mechanism with the aim of miniaturizing the orienting mechanism. The active orientation system which has two degrees of freedoms (pan and tilt) is synthesized by using a compliant mechanism. The flexible mechanisms utilize the deflection of curved beams to drive the orienting modules. A shape and size optimization process using genetic an algorithm is used for the design. The objectives of the optimization problem are to maximize the orienting angles and maximize the linearity of the linear input and angular output relation. To demonstrate the feasibility of the optimum design, finite element analysis using ABAQUS is carried out and a prototype is also fabricated using CNC laser cutting method. The experimental results show that the proposed design exhibits essential characteristics of a camera orientation a system such as lightweight, compactness and high precision.

Keywords: *Compliant mechanism; spherical mechanism; optimization; camera-orientation device; CNC laser cutting.*

1. INTRODUCTION

Autonomous vehicle guidance has received much attention from researchers because of its great potential in various applications [1-3] such as indoor security patrolling, video surveillance of indoor environments, pipe inspection robot, etc. In order to guide a vehicle to move in an unknown environment, external light source such as laser or ultrasonic sensors can be used to sketch out the topology of the surroundings. In some application, the use of either way could be harmful or uncomfortable to humans or other living creatures. In recent years, stereo vision systems gain more advantage compared to other alternatives. Stereopsis which is biologically inspired by a binocular vision from nature requires the capture of a pair of images simultaneously from different viewpoints. In computer vision, the depth information from stereopsis can be useful in object recognition, photogrammetry, or collision avoidance in mobile robotics.

Many mechanical mechanisms have been proposed to design camera-orientation devices (CODs). Commercial CODs usually use serial mechanisms with rotary motors to provide full rotation range for the camera. This kind of machine consists of several links connected in series by various types of joints, typically revolute and prismatic. It normally has one fixed link called base, and one free end called the end effector where a CCD camera can be integrated. Position analysis with inverse kinematic is usually a challenge to bring the end-effector to the desired position [4]. Furthermore, the actuator connected to the base must support the whole device, therefore, it requires a sufficiently high power to drive the mechanism.

The most desirable characteristics of a COD that is assembled into robotics are flexibility, good dynamical performance,

compactness and high accuracy [5]. To this extent, parallel kinematics is often favorable compared to the serial kinematics since only the inertial mass of the camera has to be driven and not the mass of the actuators itself [6]. To further increase the accuracy of the device by eliminating the backlash and friction presented in all traditional joints, this research proposes to use compliant mechanism (CM) to synthesize a compliant bio-inspired (CBI) camera- positioning mechanism. Compared to the traditional rigid-body mechanism, CM has numerous advantages such as reduction in part count, reduced wear and need for lubrication, light weight, increased precision since backlash is eliminated, therefore ease of miniaturizing [7].

2. WORKING PRINCIPLE

The proposed camera-orienting mechanism in this paper originates from the agile stereo pair of Samson [5] which is actually a 2 DOF spherical mechanism. A camera can be actively oriented around its vertical (pan axis) and its horizontal axes (tilt axis) (see Fig. 1 for better illustration). However, instead of using the perpendicular actuation approach, parallel actuation which is a bioinspired model of the eye plant [8] will be applied to save space for more compact arrangement in mechatronic systems (Fig. 2). In this design, two flexure beams are used to transfer the linear motions from step motors to the angular motion (pan and tilt) of the spherical mechanism. The usage of these compliant beams make the device less bulky and more accurate therefore it could be further simplified and miniaturized.

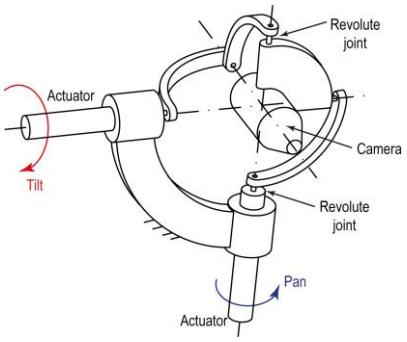

Figure 1. *A 2-DOF camera positioning device using a spherical mechanism [Samson 2006]*

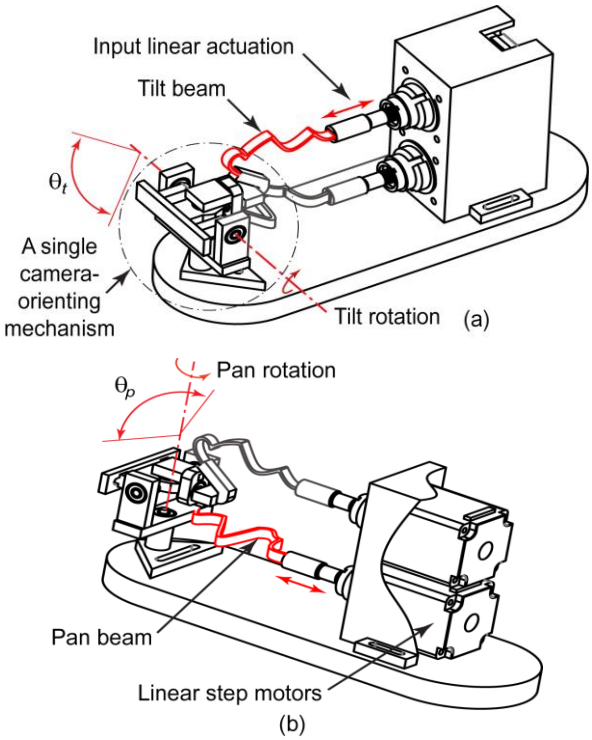

Figure 2. *Compliant tilt (a) pan (b) mechanisms to activate the COD.*

3. OPTIMIZATION DESIGN

3.1 Pan mechanism design

The pan and tilt motions are arranged in perpendicular. However, due to compactness consideration of the device, two linear step motors are arranged in parallel in order to provide these actuations. A flexural beam is used to connect the linear motor and the pan mechanism which could help to convert the linear input into an angular output. The topology of the beam will define the conversion relation whereas proportional driving is always expected due to the ease of the control system. In this research, four 3rd-order Bezier-curved segments are used to parameterize the pan beam. Fig. 3 illustrates design parameters for the pan beam where Q_{ij} $(i = 1 \div 4,\ j = 1 \div 3)$ are the control points of the Bezier curves. As described by Rogers and Adams [9], the first and last points of each Bezier curve segment are coincident with the first and last points of the defining polygon. The tangent vectors at the ends of the curve have the same directions as the first and last polygon spans, respectively. Generally, an nth order Bézier curve is

determined by $(n+1)$ control points whose general form of the curve can be represented as following [10]:

$$Q_{ij} = [x_i, y_i] \quad i = 1,2,\dots,n+1 \tag{1}$$

$$P(t) = \sum_{i=1}^{n+1} Q_{ij} b_{i,n+1}(t) \quad t \in [0,1] \tag{2}$$

$$b_{i,n}(t) = \binom{n}{i} t^i (1-t)^{n-1} \tag{3}$$

where $b_{i,n}(t)$ is Berstein polynomial, t is independent parameter, $P(t)$ and Q_{ij} denotes position vectors of points on the curve and control points, respectively.

To manipulate the pan rotation, the left-end of the pan beam is connected to the frame via point P_2. This point has shifted a distance Δ_{yp} from the horizontal line connecting the pan origin O_p and the input point of the actuator. Point P_3 will receive an input displacement from the linear motor which is then converted into the angular motion of the pan fixture via the deformation of the flexure pan beam.

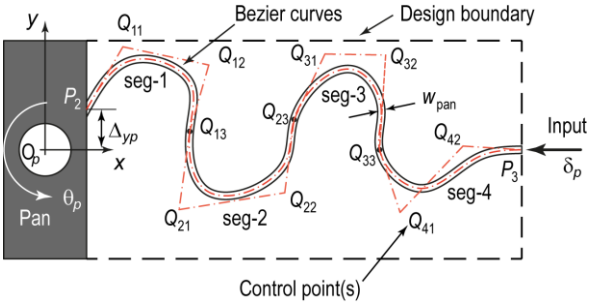

Figure 3. *Design parameters for pan beam*

A shape optimization design using FEA-based genetic algorithm was formulated for both pan and tilt beams following the procedure developed by Pham and Wang [11]. With a maximum input displacement $(\delta = \pm 9mm)$ from the linear motor, the objective functions of the optimization process are to maximize the rotation angle of the pan mechanism θ_p and maximize the linearity of the conversion relation between linear input and pan rotation output. The nondominated sorting genetic algorithm [12] is applied to the optimization of the shape and size of curved beams. This algorithm is suitable for solving multi-objective constrained nonlinear problems.

Due to the geometry complexity, large motions and flexural beam behaviors of the mechanism, the linear input displacement versus pan rotation $(\delta_p - \theta_p)$ of the device may not be calculated analytically. Finite element method can be used to analyze geometrically nonlinear behaviors of the mechanism and is also suitable to model finite axial strain and transverse shear deformation of stout as well as slender beams of the various beam geometries generated during the optimization process. Finite element analysis by a commercial software ABAQUS [13] is utilized to obtain the $(\delta_p - \theta_p)$ curve of the device. Optimization formulation for the pan beam shape design is described in Table 1. In this formulation, the objective function is described in Eq. (4) by fitting the simulated input displacement and output rotation of the pan mechanism by a linear function. The constraint function g_1 is imposed to ensure that the forward motion of the actuator will lead to a CCW rotation of the pan mechanism. The constraint g_2 seeks for a structure that is always operated in elastic limit with a safety factor (SF).

Table 1. *Formulation of pan beam optimization*

1. Objective: Given linear input $\delta_p = \pm 9mm$ – Maximize the conversion coefficient (α): $\theta_p = \alpha . \delta_p$ (4) – Maximize the linearity of $(\delta_p - \theta_p)$ function: $R^2 \to 1$
2. Design variables: – $P_2(y)$; w_{pan} – $Q_{1i}(x,y)$; $Q_{2i}(x,y)$; $Q_{3i}(x,y)$; $Q_{4i}(x,y)$ $(i = 1 \div 3)$
3. Constraints: i. g_1: $Q_{1i}(y) > P_2(y)$ $(i = 1 \div 3)$ ii. The maximum stress within the pan mechanism: g_2: $\sigma_m < \sigma_y/SF$

3.3 Tilt mechanism design

The tilt mechanism provides tilt rotation. It is also parameterized using four 3rd-order Bezier-curved segments which is illustrated in Fig. 4. Another linear actuator is used to drive the tilt mechanism. The same optimization formulation procedure for the tilt beam shape design is described in Table 2.

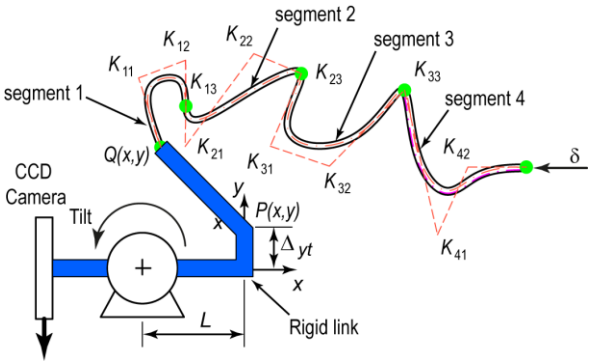

Figure 4. *Design parameters for tilt beam*

Table 2. *Formulation of tilt beam optimization*

1.*Objective*: Given linear input $\delta_t = \pm 9mm$

– Maximize the conversion coefficient (β): $\theta_t = \beta.\delta_t$ (5)

– Maximize linearity of $(\delta_t - \theta_t)$ function: $R^2 \to 1$

2.*Design variables*:

– $P(x,y)$; $Q(x,y)$; w_{tilt}

– $K_{1i}(x,y)$; $K_{2i}(x,y)$; $K_{3i}(x,y)$; $K_{4i}(x,y)$ $(i = 1 \div 3)$

3.Constraints:

i. g_1: $K_{1i}(y) > Q(y)$ $(i = 1 \div 3)$

ii. g_2: $Q(y) > P(y)$

iii. The maximum stress within the tilt mechanism: g_3: $\sigma_m < \sigma_y/SF$

In the analysis, polyoxymethylene (POM) which is considered a high performance engineering polymer with many applications in industry is used for the device. In this model, the Young's modulus (E) of POM is taken as 2.6GPa, and the Poisson's ratio (v_p) is taken as 0.25.

3.4 Optimization results

By using the GA optimization method mentioned above, optimum results for the design variables of the parameterized pan and tilt curves are presented in Table 3 and Table 4, respectively. The optimum beam element models for these two mechanisms are also presented in Fig. 5 and Fig. 6.

Table 3*. Optimum results for pan beam*

Design variables	Values (mm)
$\Delta_{yp} = \boldsymbol{P_2(y)}$	2.27
w_{pan}	0.92
$\boldsymbol{Q_{11}(x,y)}$	(4.87, 10.27)
$\boldsymbol{Q_{12}(x,y)}$	(14.21, 12.64)
$\boldsymbol{Q_{13}(x,y)}$	(11.74, 9.43)
$\boldsymbol{Q_{21}(x,y)}$	(17.85, -8.87)
$\boldsymbol{Q_{22}(x,y)}$	(21.82, 1.37)
$\boldsymbol{Q_{23}(x,y)}$	(28.38, – 6.97)
$\boldsymbol{Q_{31}(x,y)}$	(27.60, – 6.69)
$\boldsymbol{Q_{32}(x,y)}$	(36.72, – 2.08)
$\boldsymbol{Q_{33}(x,y)}$	(38.80, – 5.36)
$\boldsymbol{Q_{41}(x,y)}$	(41.19, – 10.84)
$\boldsymbol{Q_{42}(x,y)}$	(46.57, – 9.14)

Table 4*. Optimum results for tilt beam*

Design variables	Values (mm)
P(x,y)	(0, 5.13)
Q(x,y)	(–11.39, 10.35)
w_{tilt}	0.81
$K_{11}(x,y)$	(– 11.78, 19.92)
$K_{12}(x,y)$	(– 6.93, 17.03)
$K_{13}(x,y)$	(– 3.21, 19.70)
$K_{21}(x,y)$	(– 2.69, 18.34)
$K_{22}(x,y)$	(4.96, 6.44)
$K_{23}(x,y)$	(1.78, 17.31)
$K_{31}(x,y)$	(8.10, 16.40)
$K_{32}(x,y)$	(10.58, 16.79)
$K_{33}(x,y)$	(13.26, 16.72)
$K_{41}(x,y)$	(16.65, 9.85)
$K_{42}(x,y)$	(16.84, 11.50)

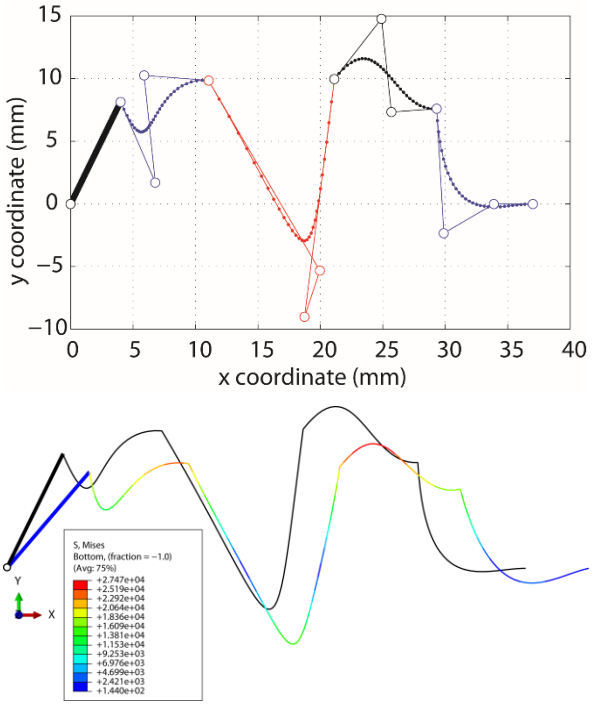

Figure 5. *Optimum pan beam deformation simulation*

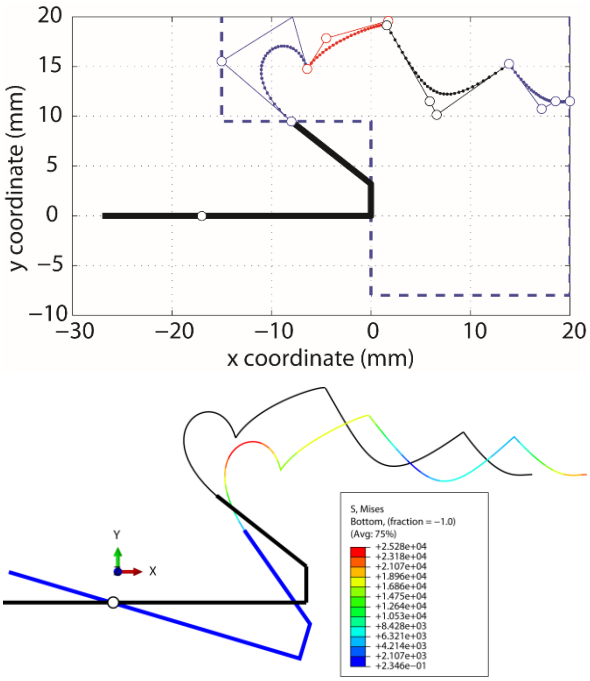

Figure 6. *Optimum tilt beam deformation simulation*

The driving force and maximum stress built up within the tilt beam are also illustrated in Fig. 7. Generally, for the forward motion of the motors which leads to the compression of the beams, the reaction force is smaller than that of the reverse motion. It shows an unsymmetrical pattern for the force diagram. In order to alleviate failure of the mechanism, maximum stress should be maintained lower than the yield strength of the material ($\sigma_y = 76MPa$).

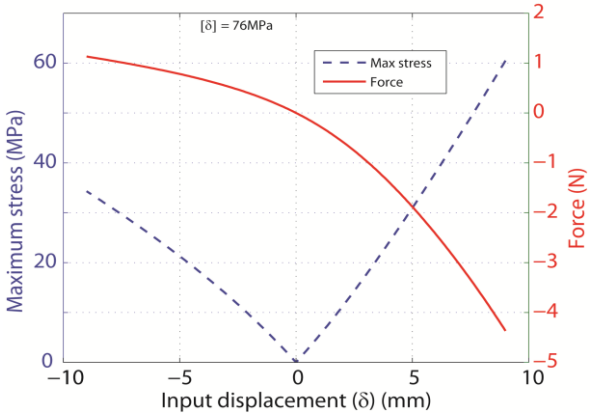

Figure 7. *Force and maximum stress of the tilt beam*

The most important requirement for the design of the COD is the symmetry of the angle rotation versus input displacement diagram for both pan and tilt mechanisms. The angle rotation versus input displacement diagram for these optimum mechanisms is simulated as shown in Fig. 8. Linear regression is used to fit the simulation results. Fig. 8 shows a rather good fit for both mechanisms. The largest pan angle is 28.1^o and the largest tilt angle is 27.6^o when the maximum input displacement is ±9mm. The fitted pan and tilt relation for the optimum designs are described as following:

$$\theta_p = -3.06\delta_p \quad (6)$$

$$\theta_t = 3.28\delta_t \quad (7)$$

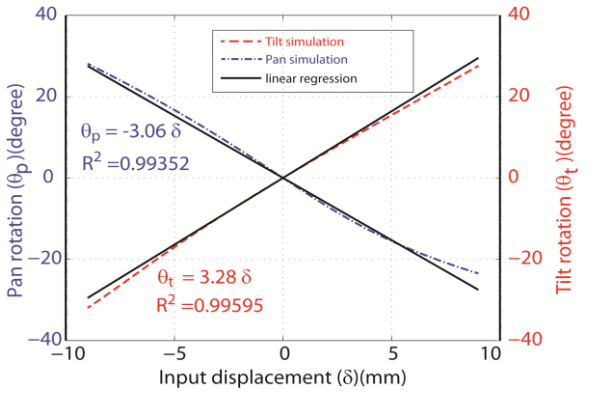

Figure 8. *Pan and tilt angle rotation vs. linear input*

4. FABRICATION AND EXPERIMENTS

The pan and tilt beams are fabricated by using CNC laser cutting technology (Laser TR-1390) from the POM material. Their dimensions are based on the optimal parameters obtained from the optimization process. They are then assembled with other components to make a complete CBI camera-positioning mechanism as shown in Fig. 9. To separately drive the mechanisms, linear step motors (Haydon 21H4AC – 7.5-A04, Haydonkerk Motion Solutions) that have an overall dimension of 20x20x40mm and a 2.0mm lead per revolution could provide a 0.01mm input displacement step. Although the size of the linear actuators is small, it still can provide a large enough thrust force (up to 45N) to overcome the reaction force created by the compression/ tension of the pan and tilt beams. The inset (a) in Fig. 9 shows a picture of the motor. Fig. 10 shows the operation of the device while it is independently rotated the pan and tilt axis.

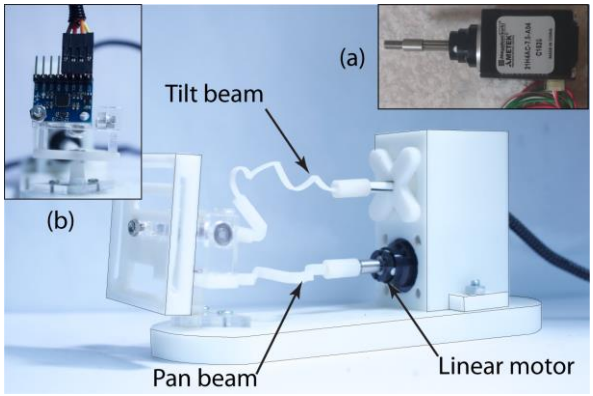

Figure 9. *Fabricated device*

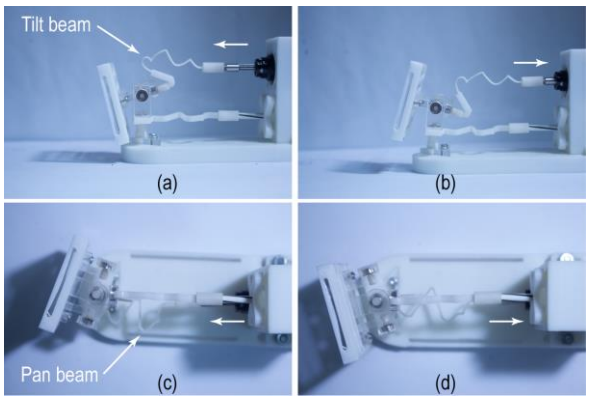

Figure 10. *Tilt (a-b) and pan (c-d) operation*

In order to measure the rotation angle of a pan and tilt axis, an integrated 6-axis MotionTracking sensor (MPU– 6050, InvenSense Inc.) that combines a 3-axis gyroscope, 3-axis accelerometer and a Digital Motion Processor™ (DMP) all in a small 4x4x0.9mm package is integrated to the device. The inset (b) in Fig. 9 shows this sensor. It is connected to an Arduino Uno circuit to record the rotation angle data. The relation between rotation angle and linear input displacement of both pan and tilt axis is illustrated in Fig. 11. The measured value is slightly smaller compared to the simulated results for both axes. This discrepancy can be attributed to the uncertainties in material properties, geometry and loading conditions of the experiments. The fabricated mechanism also has slightly smaller beam widths than the designed value due to the manufacturing error in the laser cutting process.

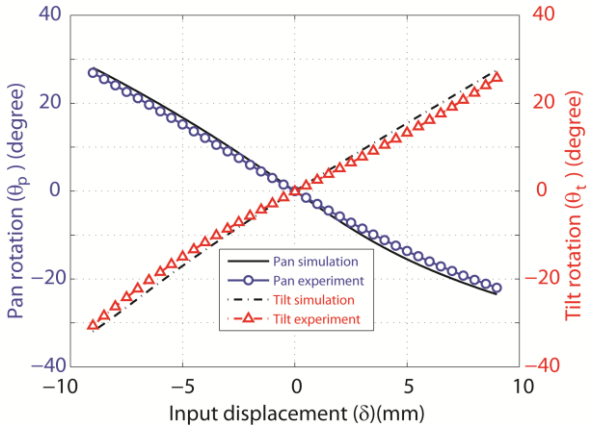

Figure 11. *Experimental results of pan and tilt rotation*

The designed and fabricated COD is finally encapsulated in a housing and assembled into the platform of an AGV robot as shown in Fig. 12. This robot consists of a vehicle which has a commercial pcDuino test bed developed by Chen [14]. It is supported by ASU VIPLE programming environment which is an IoT based visual programming language. Beside an ultrasonic sensor (HC-RS04) that is used for short-range sensing on the right-hand side, the camera orienting device is used to observe the front view of the vehicle.

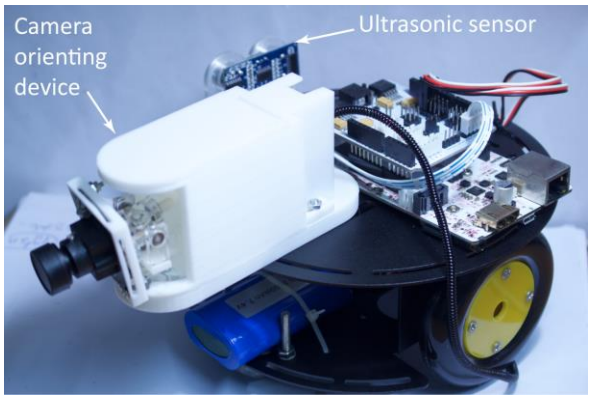

Figure 12. *Integrated the device to an autonomous vehicle*

5. CONCLUSIONS

In this research, we have proposed the design of a compliant bio-inspired camera-positioning mechanism. Shape optimization coupled with genetic algorithm has been used during the design process. Using the designed methodology, optimum shape of pan and tilt mechanisms were found. Their operation has been verified by FEA and experiment. A prototype is also fabricated using the CNC laser cutting method. Taking full advantage of compliant mechanisms, without movable joints, the use of the designed device would results in reduced wear, reduced need for lubrication and increased performance by increasing precision.

ACKNOWLEDGMENTS

The authors are thankful for the financial support from the HCMC University of Technology and Education (HCMUTE), under Grant No. T2018-04TĐ.

REFERENCES

[1] K.C. Chen and W.H. Tsai, "Vision-based autonomous vehicle guidance for indoor security patrolling by a sift-based vehicle-localization technique," *IEEE Transactions on Vehicular Technology*, vol. 59(7), pp. 3261-3271, 2010.

[2] C. Micheloni, G. L. Foresti, C. Piciarelli, and L. Cinque, "An autonomous vehicle for video surveillance of indoor environments," *IEEE Trans. Veh. Technol.*, vol. 56, no. 2, pp. 487–498, 2007.

[3] M. Hoshina, T. Mashimo, and S. Toyama, "Development of spherical ultrasonic motor as a camera actuator for pipe inspection robot," *in Proc. IEEE/RSJ Int. Conf. Intell. Robot Syst*., St. Louis, MO, pp. 2379–2384, 2009.

[4] Z. Pandilov, V. Dukovski, "Comparison of the characteristics between serial and parallel robots", *Acta Technica Corvininesis - Bulletin of Engineering*, Vol. 7 Issue 1, pp. 143-160, 2014.

[5] E. Samson, et al., "The agile stereo pair for active vision," *Machine Vision and Applications*, vol. 17, pp. 32-50, 2006.

[6] Villgrattner, T. and H. Ulbrich, "Design and control of a compact high-dynamic camera-orientation system." *IEEE/ASME Transactions on Mechatronics* 16(2): 221-231, 2011.

[7] L.L. Howell, *Compliant Mechanisms*, John Wiley & Sons, New York, 2002.

[8] Cannata, G. and M. Maggiali "Models for the design of bio-inspired robot eyes." *IEEE Transactions on Robotics* 24(1): 27-44, 2008.

[9] D.F. Rogers, J.A. Adams, *Mathematical Elements for Computer Graphics*, 2nd ed., McGRAW-Hill, New York, 1990.

[10] D. Salomon, *Curves and Surfaces for Computer Graphics*, Springer, New York, 2006.

[11] H.T. Pham, and D.A. Wang, "A quadristable compliant mechanism with a bistable structure embedded in a surrounding beam structure," *Sensors and Actuators A – Physical*, vol. 167, pp. 438-448, 2011.

[12] Deb K, Pratap A, Agarwal S, Meyarivan T., "A fast and elitist multiobjective genetic algorithm: NSGA-II," *IEEE Transactions on Evolutionary Computation*, vol. 6, pp. 182–197, 2002.
[13] Hibbitt HD et al., *ABAQUS User Manual*, Version 6-2, HKS Inc., Providence, RI, USA, (2001).
[14] Y. Chen, "Analyzing and visual programming Internet of Things and autonomous decentralized systems," *Simulation Modelling Practice and Theory*, vol. 65, pp. 1-10, 2016.

Corresponding author:
Pham Huy Tuan
Ho Chi Minh City University of Technology and Education
Email: phtuan@hcmute.edu.vn